Cellular and Molecular Life Sciences (2025) 82:246
https://doi.org/10.1007/s00018-025-05760-3

ORIGINAL ARTICLE

THAP11-mediated K48- and K63-linked ubiquitination is essential for the degradation of porcine reproductive and respiratory syndrome virus nonstructural protein 1β

Binghua Chen[1,2] · Yongsheng Xie[3] · Zhan He[1] · Yongjie Chen[1] · Jiecong Yan[1] · Fangfang Li[1] · Yunyan Luo[1] · Yanfei Pan[1] · Min Liu[1] · Chunhe Guo[1]

Received: 26 February 2025 / Revised: 14 May 2025 / Accepted: 16 May 2025

Abstract

Porcine reproductive and respiratory syndrome virus (PRRSV) is a highly infectious pathogen in the global pig industry that causes significant economic losses. Owing to its rapid mutation, effective antiviral treatments or vaccines are still lacking. Therefore, it is essential to identify potential host factors that interact with PRRSV-encoded proteins. In this study, a porcine alveolar macrophage cDNA library was used to identify host proteins that interact with PRRSV nonstructural protein 1β (Nsp1β) via a yeast two-hybrid system. A total of 34 potential host factors were identified, with Thanatos-associated protein 11 (THAP11) strongly interacting with Nsp1β. These interactions were further analyzed via Gene Ontology (GO) and Kyoto Encyclopedia of Genes and Genomes (KEGG) pathway analyses. Co-localization of Nsp1β with THAP11, poly(rC)-binding protein 1 (PCBP1), thioredoxin-interacting protein (TXNIP), and cathepsin D (CTSD) was observed, and co-IP assays confirmed the Nsp1β-THAP11 interaction. The overexpression of THAP11 reduced PRRSV N protein accumulation, indicating an antiviral effect, whereas the silencing of THAP11 increased PRRSV replication. Furthermore, THAP11 promoted the degradation of Nsp1β by increasing K48- and K63-linked ubiquitination, thereby restricting PRRSV replication. These findings suggest that THAP11 exerts an antiviral effect by interacting with and degrading Nsp1β via the ubiquitin-proteasome system, providing insights for future PRRSV defence strategies.

Keywords Yeast two-hybrid screening · Virus-host interactions · PRRSV · Nsp1β · THAP11

Introduction

Porcine reproductive and respiratory syndrome (PRRS) is one of the most devastating diseases in the global pig industry, leading to significant economic losses worldwide [1]. It is caused by the porcine reproductive and respiratory syndrome virus (PRRSV), which severely affects the reproductive health of sows and the respiratory health of piglets [2]. This disease results in reduced productivity and substantial economic burdens on pig farming. PRRSV is characterized by rapid mutation and high genetic variability, which makes it particularly difficult to control with existing vaccines and antiviral therapies [3–7]. Consequently, new research aimed at identifying critical host-virus interactions and discovering novel antiviral targets is essential for improving PRRS management and treatment [8, 9].

PRRSV is a single-stranded, positive-sense RNA virus that is approximately 15 kilobases (kb) in length. It belongs

Binghua Chen, Yongsheng Xie and Zhan He contributed equally to this work.

✉ Chunhe Guo
guochunh@mail.sysu.edu.cn

1 Guangdong Laboratory for Lingnan Modern Agriculture, State Key Laboratory for Animal Disease Control and Prevention, Key Laboratory of Zoonosis Prevention and Control of Guangdong Province, College of Veterinary Medicine, South China Agricultural University, Guangzhou, Guangdong, PR China

2 College of Henry Fork School of Biology and Agriculture, Shaoguan University, Daxue Road, Zhenjiang District, Shaoguan 512005, China

3 College of Life Science and Resources and Environment, Yichun University, Yichun 336000, Jiangxi, China

Published online: 23 June 2025

to the family *Arteriviridae* and contains 10–12 open reading frames (ORFs) encoding several nonstructural (Nsp1-Nsp12) and structural proteins (GP2a, E, GP3, GP4, GP5, M and N) [10, 11]. PRRSV is known to inhibit type I interferon responses through nonstructural proteins (Nsp1α, Nsp1β, Nsp2, Nsp4 and Nsp11) [12–18]. Nonstructural protein 1β (Nsp1β) is a key nonstructural protein encoded by PRRSV. As an essential viral protein, Nsp1β plays a critical role in the pathogenesis of PRRSV by modulating the host immune response and assisting the virus in evading immune detection [19–21]. The protein is encoded by the PRRSV genome as part of the viral replicase complex, responsible for viral RNA replication and transcription [20, 22].

The functional analysis of Nsp1β has focused primarily on its immune evasion mechanisms, as this is a critical factor in PRRSV pathogenesis. Early studies demonstrated that Nsp1β interferes with interferon signaling by preventing the activation of the interferon regulatory factor 3 (IRF3) pathway [19, 23], inhibiting the production of type I interferons, which are typically induced upon viral infection as part of the host's early antiviral responses. Further studies have shown that Nsp1β may also directly interact with other components of the innate immune system. For example, Nsp1β has been reported to interact with the host's cellular RNA-sensing pathways, preventing the host from detecting viral RNA effectively [14, 20, 23]. It inhibits the JAK-STAT pathway by preventing the nuclear translocation of STAT1 and STAT2, which are essential for initiating interferon (IFN) responses [24, 25]. This blockade significantly hinders the host's ability to mount an effective immune defence, allowing the virus to evade immune recognition.

Furthermore, Nsp1β binds to nucleoporin 62 (Nup62), a component of the nuclear pore complex, to block the nuclear export of antiviral mRNAs and proteins. This action impairs the host's capacity to produce antiviral proteins, further contributing to the virus's ability to replicate unchecked [26]. Additionally, Nsp1β stabilizes its protein form by interacting with host deubiquitinating enzymes, such as ubiquitin-specific proteinase 1 (USP1), preventing its degradation through the ubiquitin-proteasome pathway [27]. This stabilization not only preserves Nsp1β's ability to suppress immune responses but also promotes viral replication. Nsp1β also stabilizes hypoxia-inducible factor 1 alpha (HIF-1α), a key regulator of inflammation, through deubiquitination. This process enhances viral replication by promoting inflammation and modulating immune responses to favor virus survival [28]. Moreover, Nsp1β inhibits the activation of the NLRP3 inflammasome, a crucial player in triggering inflammatory responses. This inhibition further suppresses the host's immune response, facilitating viral persistence [29]. Nsp1β also interacts with host proteins such as the DEAD-box RNA helicase DDX21 (DDX21) and GTPase-activating protein SH3 domain-binding protein 1 (G3BP1), which regulate viral replication and stress granule dynamics [30, 31]. These interactions help modulate the host cellular environment to favor viral replication while avoiding immune detection. Finally, Nsp1β induces the degradation of karyopherin α1 (KPNA1), a key molecule involved in the nuclear import of immune signaling complexes such as interferon-stimulated gene factor 3 (ISGF3) [24]. By disrupting the nuclear translocation of these complexes, Nsp1β effectively inhibits host immune responses, further enhancing viral replication. In summary, Nsp1β uses multiple mechanisms, including the disruption of immune signaling pathways, the stabilization of key host factors, and interference with antiviral mRNA export, to create a favorable environment for PRRSV replication and immune evasion.

Thanatos-associated protein 11 (THAP11) is a transcriptional regulator containing a highly conserved THAP domain [32]. THAP11 has been implicated in regulating apoptosis, oxidative stress, and immune responses, making it a potential factor in viral infections. The THAP domain is found in a variety of proteins involved in cellular stress responses and DNA repair, and THAP11 itself is known to interact with key host proteins to control cellular processes such as cell survival and inflammation [33–37]. While the role of THAP11 in cellular processes is well-documented, its involvement in viral infections, particularly PRRSV infection, has not been thoroughly studied. Given the ability of THAP11 to modulate immune responses and its role in cellular stress pathways, THAP11 may play a role in the host's defence against viral infections, including PRRSV. While poly(rC)-binding protein 1 (PCBP1) is a multifunctional RNA-binding protein that plays diverse roles in viral infections through kinds of primary mechanisms [38–43], thioredoxin-interacting protein (TXNIP) has emerged as a critical regulator of viral pathogenesis through its involvement in multiple antiviral pathways [44–46], and cathepsin D (CTSD), a key lysosomal protease, contributes to viral infection cycles via several established mechanisms [47], which all have been reported to be related to the virus infections.

In this study, we utilized a porcine alveolar macrophage (PAM) cDNA library and a yeast two-hybrid system to screen for host proteins that interact with PRRSV Nsp1β. A total of 34 potential interacting host proteins were identified. Among these, THAP11 demonstrated a particularly strong interaction with Nsp1β, making it a prime candidate for further investigation. Co-localization experiments, as well as co-IP assays, confirmed the interaction between Nsp1β and THAP11. Furthermore, the overexpression of THAP11 resulted in a significant reduction in PRRSV N

protein accumulation, suggesting that THAP11 exerts an antiviral effect by inhibiting PRRSV replication.

On the other hand, silencing THAP11 enhanced PRRSV replication, indicating that THAP11 plays a critical role in controlling viral replication. Further mechanistic studies revealed that THAP11 promotes the degradation of Nsp1β through the ubiquitin-proteasome system, specifically by enhancing K48- and K63-linked ubiquitination. These findings suggest that THAP11 functions not only as a regulatory protein but also as an important factor in the degradation of Nsp1β, thereby limiting the ability of the virus to evade immune detection and replicate efficiently. These results highlight THAP11 as a novel antiviral host factor in PRRSV infection, providing a potential target for the development of new antiviral strategies.

This study contributes to the growing body of knowledge on host-virus interactions in PRRSV infection and provides new insights into the role of THAP11 in modulating viral replication through the ubiquitin-proteasome system. Understanding how PRRSV manipulates host proteins, such as THAP11, to evade immune detection and promote replication could pave the way for the development of more effective antiviral therapies and vaccines.

Materials and methods

Plasmids and cell lines

The bait plasmid for the yeast library screen was constructed via a traditional method. The cDNA encoding Nsp1β from the classical CH-1a strain of PRRSV-2 subtype 2 was amplified via PCR with the specific primers listed in Supplemental Table S1. The amplified product was then cloned and inserted into the yeast pGBKT7 vector via *EcoRI* and *BamHI* restriction sites to express the Gal4 DNA-binding domain fusion protein.

The cDNA library for PAMs was constructed via SMART technology and subsequently cloned and inserted into the pGADT7-Rec vector via gene recombination techniques. The full-length cDNA sequence of the gene of interest was synthesized via reverse transcription PCR (RT-PCR) and then cloned and inserted into the pGADT7 yeast vector with *EcoRI* and *XhoI* restriction sites added to the primers listed in Supplemental Table S1.

Marc-145 and HEK293 T cells were obtained from previous laboratory stocks and cultured in Dulbecco's modified Eagle's medium (Gibco, NY, USA) supplemented with 10% fetal bovine serum. All the cells were maintained at 37 °C in a 5% CO_2 incubator. All the experiments were performed at the Level 2 Biosafety Laboratory at the College of Veterinary Medicine, South China Agricultural University.

Yeast two-hybrid (Y2H) assays

In Y2H assays, a PAM cDNA library for *Sus scrofa* was constructed to screen for proteins that interact with PRRSV Nsp1β via the GAL4 system as described in the BD Matchmaker Library Construction and Screening Kits User Manual (Clontech, Palo Alto, CA). Nsp1β was cloned and inserted into the yeast pGBKT7 vector and used as bait by cotransformation into Y2H Gold yeast cells with the PAM cDNA library. The transformants were subsequently grown on SD/-Leu/-Trp/-His media (TDO), and positive clones were selected on Ade/Leu/Trp/His-deficient media and then confirmed via 5-Br-4-Cl-3-indoxyl α-D-galactoside (X-α-Gal) and aureobasidin A (AbA)/(QDO/X/A) assays. To confirm the interaction between proteins, full-length sequences of host protein were fused into the pGADT7 vector (Clontech, Palo Alto, CA) as prey. The corresponding PRRSV proteins were subjected to Y2H assays. Transformants were plated on synthetic defined media lacking Leu and Trp (SD/-Leu/-Trp, DDO), grown for three days, and then transferred to synthetic defined media lacking Ade, Leu, Trp and His supplemented with 70 μg/ml X-α-Gal and AbA (SD/-Ade/-Leu/-Trp/-His/X-α-Gal, QDO/X/A). Positive control experiments were performed by co-transforming pGBK-53 and pGAD-T, while negative controls were performed with pGBK-Lam and pGAD-T. Three independent experiments were conducted to confirm the results.

Detection of autoactivation and toxicity

BD-Nsp1β and the empty pGADT7 vector were cotransformed into Y2H cells. The transformants were then plated onto DDO/X, TDO/X, and QDO/X/AbA selective media for screening.

Confocal microscopy

HEK293 T cells were cultured in 12-well plates containing 20 mm polylysine-coated coverslips. When the cells reached 70–80% confluence, they were cotransfected with plasmids expressing Nsp1β and THAP11 or appropriate controls. At 24 h posttransfection (hpt), the cells were processed for immunofluorescence (IF) staining according to standard procedures. Finally, the polylysine-coated coverslips were mounted onto glass slides via nail polish. Fluorescence images were captured via a confocal fluorescence microscope (Leica, Germany) [48].

Western blot analysis

Cell samples cultured in 6-well or 12-well plates were lysed with RIPA buffer (high) (Solarbio) according to the

manufacturer's protocol. The lysates were subjected to ultrasonic disruption and then centrifuged at 12,000 rpm for 10 min (min). The resulting supernatant was collected in 500 µL sterile tubes, combined with 5×SDS-PAGE loading buffer, heated at 100 °C for 10 min, and cooled on ice for 2 min. Protein separation was performed via SDS-polyacrylamide gel electrophoresis (SDS-PAGE) via the One-Step PAGE Gel Fast Preparation Kit (Vazyme Biotechnology, China). The proteins were subsequently transferred to a PVDF membrane via semidry transfer. After the membrane was blocked with a solution containing 5% nonfat dry milk and 0.1% Tween 20 for 1 h at room temperature, it was incubated with specific primary or endogenous antibodies overnight at 4 °C. Next, the membrane was incubated with an HRP-conjugated anti-mouse/rabbit IgG secondary antibody for 1 h at room temperature. Finally, the protein bands were visualized via an Amersham ImageQuant 800 (Cytiva, Washington, DC, USA).

Coimmunoprecipitation (Co-IP) assays

Magnetic beads conjugated with anti-Myc or anti-mCherry antibodies were prepared following the instructions provided in the Protein A/G immunoprecipitation Kit (Selleck). For the co-IP assay, cells cultured in 6-well plates were lysed for 30 min on ice with 250 µL of cell lysis buffer (Beyotime) supplemented with 1 mM PMSF protease inhibitor. The lysates were disrupted via ultrasonic treatment and centrifuged at 12,000 rpm for 15 min. A small aliquot of the supernatant was collected for input detection, while the remainder was incubated with protein A/G magnetic beads (Selleck) for antibody binding, according to the manufacturer's protocol. The antigen-antibody complexes were incubated for 2 h at room temperature, and the beads were washed five times with washing buffer (50 mM Tris, 150 mM NaCl, 0.5% detergent, pH 7.5). To elute the proteins, 40 µL of 1×SDS-PAGE loading buffer was added to the beads, followed by denaturation at 100 °C for 5 min. The proteins were then separated by SDS-PAGE for detection.

Immunofluorescence (IFA) assays

The cells were fixed in 4% paraformaldehyde for 15 min, followed by permeabilization with 0.5% Triton X-100 for 5 min. After being blocked with 1% BSA for 1 h at room temperature, the cells were incubated with primary antibodies overnight. Following washes, the cells were exposed to secondary antibodies conjugated with Alexa Fluor 488 or 555 fluorochromes (Cell Signaling Technology) for 1 h at room temperature. After further washing, the cells were stained with DAPI (Beyotime, China) for 5 min. Finally, fluorescence images were captured via an inverted microscope (Nikon ECLIPSE Ti2).

Quantitative RT-PCR (qPCR)

Total RNA was extracted from Marc-145 cells via TRIzol reagent. First-strand cDNA was synthesized via reverse transcription polymerase chain reaction (RT-PCR). Subsequently, quantitative PCR (qPCR) was performed using ChamQ SYBR qPCR Master Mix (Low ROX Premixed) (Vazyme, Nanjing, China) following the manufacturer's instructions.

Plasmid transfection and RNA interference (RNAi)

HEK293 T or Marc-145 cells were grown in 6/12-well plates at 80% confluence, and the different recombinant plasmids were separately transfected or cotransfected into the cells via the transfection reagents polyethylenimine (PEI) or Lipofectamine 2000. Two small interfering RNAs (siRNAs) targeting the THAP11 gene coding sequence (CDS) region were designed and ordered by SYNBIO Technologies, Suzhou, China (Supplemental Table S1). siTHAP11-1 and siTHAP11-2 or negative control (siNC) were transfected into Marc-145 cells via the Lipofectamine 2000 transfection reagent. At 24 hpt, the cells were harvested for analysis of THAP11-knockdown efficiency through real-time PCR and western blotting.

Functional enrichment analysis of interacting proteins

GO enrichment and KEGG pathway enrichment analyses against screened interacting proteins were conducted via the Metascape website (https://metascape.org/gp/index.html), and enriched data were visualized via a bioinformatics website (https://www.bioinformatics.com.cn/).

Alphafold3 predict protein structure

In this study, the three-dimensional structures of target proteins were predicted using AlphaFold3 (https://alphafold3.org/), a state-of-the-art protein structure prediction platform, based on their respective amino acid sequences.

Statistical analysis

In this study, assays were conducted with at least three independent replications per the instruction manual. The qPCR experiments were performed via the QuantStudio 3 Real-Time PCR System (Thermo Fisher, USA), and the data were analyzed via GraphPad Prism software (version 8.0).

Statistical analyses were carried out via Student's *t*-test and one-way ANOVA. Differences with *P*-values less than 0.05 were considered statistically significant.

Results

PRRSV Nsp1β does not exhibit self-activation in Y2H screening assays

Nsp1β serves as a critical interferon inhibitor during PRRSV infection. To identify host factors that interact with Nsp1β, the full-length sequence of Nsp1β was inserted into the yeast library bait vector pGBKT7. The pGBKT7-Nsp1β plasmid was cotransformed with the pGADT7-T plasmid into Y2H Gold cells, which were subsequently cultured on selective media with varying nutritional deficiencies. The cotransformed cells produced only a few clones on TDO selective medium supplemented with X-α-gal (TDO/X), but no clones were observed on QDO/X medium supplemented with AbA (QDO/X/A) (Fig. 1A). Under these conditions, Y2H screening assays using pGBKT7-Nsp1β as bait were performed on the most stringent QDO/X/A media, which presented the highest level of nutritional deficiency (Fig. 1B).

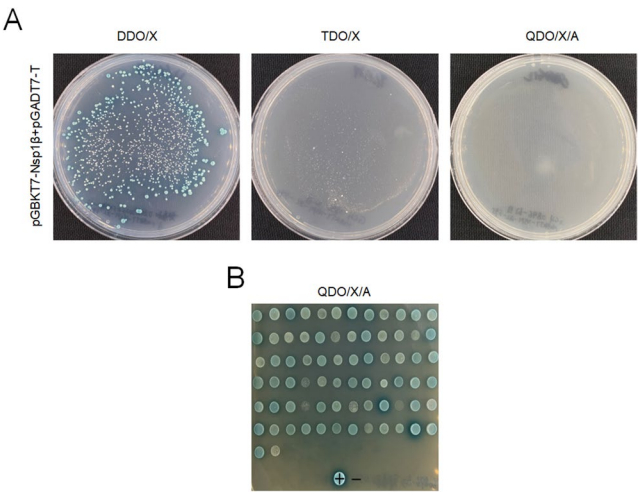

Fig. 1 Detection of self-activation of the PRRSV Nsp1β protein via Y2H screening assays. **(A)** The pGBKT7-Nsp1β and pGADT7-T plasmids were cotransformed into Y2H Gold cells, which were then plated onto deficient culture media lacking Leu and Trp (DDO/X); Leu, Trp, and His (TDO/X); and Leu, Trp, His, and Ade (QDO/X/A), supplemented with X-α-gal and AbA. **(B)** Potential positive clones that interact with Nsp1β were screened on QDO/X/A media. The blue colonies indicate positive interactions, with "+" representing a positive result and "−" indicating a negative result

Thirty-four potential host proteins that interact with Nsp1β were identified

To screen for host proteins that interact strongly with Nsp1β, bait plasmids and prey (cDNA library) were cotransformed into Y2H Gold cells, which were then cultured on stringent TDO/X medium plates. A total of 74 clones were grown on the QDO/X/A medium plates, which were further tested for interactions. Positive transformants were identified through sequencing, revealing 34 potential binding partners of Nsp1β, as listed in Table 1, including THAP11, PSMB10, PCBP1, TXNIP, and CSTD. To understand the interrelationships among candidate interacting proteins, the protein-protein interaction (PPI) network analysis revealed extensive connectivity among the identified host factors, including direct and indirect interactions between CTSD, PSMB10, TXNIP, PCBP1, and other proteins. Notably, THAP11 formed no detectable connections with any other nodes in the network (Fig. 2A). This striking topological segregation suggests that while most proteins function within collaborative networks, THAP11 may operate through unique, independent mechanisms, highlighting the coexistence of functional diversity and singularity in host-virus interactions.

Co-localization of Nsp1β with multiple host proteins

To better visualize the interactions between Nsp1β and PCBP1, TXNIP, and CSTD in vivo, the full-length sequence of Nsp1β was inserted into the pCAGGS expression vector with a C-terminal fusion to the mCherry tag. The open reading frames of PCBP1, TXNIP, and CSTD were separately cloned and inserted into the pcDNA3.1 vector, with a C-terminal fusion to the Myc tag. At 24 hpt, Nsp1β-mCherry with host proteins and pcDNA3.1-Myc were used as negative controls, and indirect IFA was performed to assess the co-localization of Nsp1β with the selected host proteins. Confocal fluorescence microscopy was used to observe the subcellular localization patterns. The results revealed that PRRSV Nsp1β was predominantly expressed in the nucleus. Cotransfection of Nsp1β-mCherry with each of the four host proteins resulted in merged yellow fluorescence, indicating co-localization, whereas cotransfection of the empty vector with Nsp1β-mCherry resulted in only single fluorescence (Fig. 2B). These findings suggest that Nsp1β colocalizes with selected host proteins.

GO enrichment and KEGG pathway enrichment analysis

To investigate the role of Nsp1β in regulating host cell metabolism, immune responses, and self-replication

Table 1 Information concerning potential host factors that interact with PRRSV Nsp1β

No	ID	Name	Gene symbol
1	NP_001038079.1	thioredoxin-interacting protein	TXNIP
2	NP_001038030.1	proteasome subunit beta type-10	PSMB10
3	AAY42145.2	cathepsin D	CTSD
4	XP_020922421.1	probable ATP-dependent RNA helicase DDX5 isoform X3	DDX5
5	XP_013843801.1	L-lactate dehydrogenase B chain isoform X1	LDHB
6	XP_005655974.2	persulfide dioxygenase ETHE1, mitochondrial	ETHE1
7	NP_001229990.1	alpha-actinin-1	ACTN1
8	XP_003125105.1	poly(rC)-binding protein 1	PCBP1
9	NP_001090927.1	cathepsin B precursor	CTSB
10	NP_001233111.1	THAP domain-containing protein 11	THAP11
11	XP_003124995.1	macrophage-capping protein	CAPG
12	XP_003127414.1	ER membrane protein complex subunit 10 isoform X1	EMC10
13	XM_021090073.1	sortilin 1, transcript variant X4, mRNA	SORT1
14	XP_013854598.1	folate receptor 1 isoform X2	FOLR1
15	XP_020936382.1	filamin-A isoform X1	FLNA
16	NP_001072147.1	CD81 molecule	CD81
17	XP_020922821.1	acyl-CoA synthetase family member 2, mitochondrial isoform X2	ACSF2
18	ABC17921.1	MHC class I antigen	SLA
19	XP_003123039.1	ATP synthase subunit delta, mitochondrial	ATP5D
20	NP_001278705.1	macrosialin precursor	CD68
21	XP_020936879.1	apical endosomal glycoprotein isoform X7	MAMDC7
22	XP_005660860.1	ferritin heavy chain isoform X1	FTH1
23	XP_005669190.1	myb-binding protein 1 A isoform X2	MYBBP1 A
24	XP_001927370.3	beta-1,4-galactosyltransferase 3	B4GALT3
25	NP_001027548.1	hypoxanthine-guanine phosphoribosyltransferase	HPRT1
26	XP_020936398.1	filamin-A isoform X11	FLNA
27	NP_999066.1	propionyl-CoA carboxylase beta chain, mitochondrial precursor	PCCB
28	XP_001929153.1	TOX high mobility group box family member 4	TOX4
29	XP_020940051.1	docking protein 3	DOK3
30	XP_020942955.1	SH2 domain-containing protein 6	SH2D6
31	XM_005660642.3	lysine acetyltransferase 5	KAT5
32	XP_020939148.1	microtubule-associated serine/threonine-protein kinase 3	MAST3
33	XM_021080945.1	putative GTP-binding protein 6	GTPBP6
34	NP_001230636.1	cytosolic nonspecific dipeptidase 2	CNDP2

processes through interactions with host factors, Gene Ontology (GO) functional analysis and Kyoto Encyclopedia of Genes and Genomes (KEGG) pathway enrichment analyses were performed on the 34 identified interacting proteins. GO cellular component analysis revealed enrichment in the lytic vacuole, mitochondrial matrix, and melanosome (Fig. 2C). GO molecular function analysis revealed that proteins interacting with Nsp1β were associated with cell adhesion molecule binding, ligase activity, and integrin binding, whereas some were involved in regulating DNA binding, receptor activity, and enzyme activity (Fig. 2D). GO biological process analysis revealed enrichment in the enzyme-linked receptor protein signaling pathway, cellular metabolism, regulation of biosynthetic processes, and antiviral immune responses (Fig. 2E). KEGG pathway analysis revealed that the interacting host proteins were involved primarily in cell growth and death, transport and catabolism, the host immune system, and signal transduction (Fig. 2F). In conclusion, PRRSV Nsp1β may evade host immune responses by interacting with various cellular signaling molecules and pathways.

THAP 11 interacts with Nsp1β in vivo and in vitro

Among the screened proteins, genes with a nucleotide length of less than 2000 bp were selected as potential study targets. In the yeast assay, a strong interaction between Nsp1β and THAP11 was observed on QDO selective media supplemented with X-α-gal and AbA (QDO/X/A) (Fig. 3A). Next, the full-length of THAP11 sequence from *Chlorocebus sabaeus* was cloned and inserted into the pcDNA3.1 expression vector and fused with a C-terminal Myc tag. The Nsp1β sequence from the classical PRRSV CH-1a strain was inserted into the pCAGGS-mCherry expression vector, with a C-terminal fusion to the mCherry tag. HEK293 T cells were cotransfected with THAP11-Myc and Nsp1β-mCherry for 24 h, followed by incubation with either an anti-mCherry antibody or a control IgG antibody.

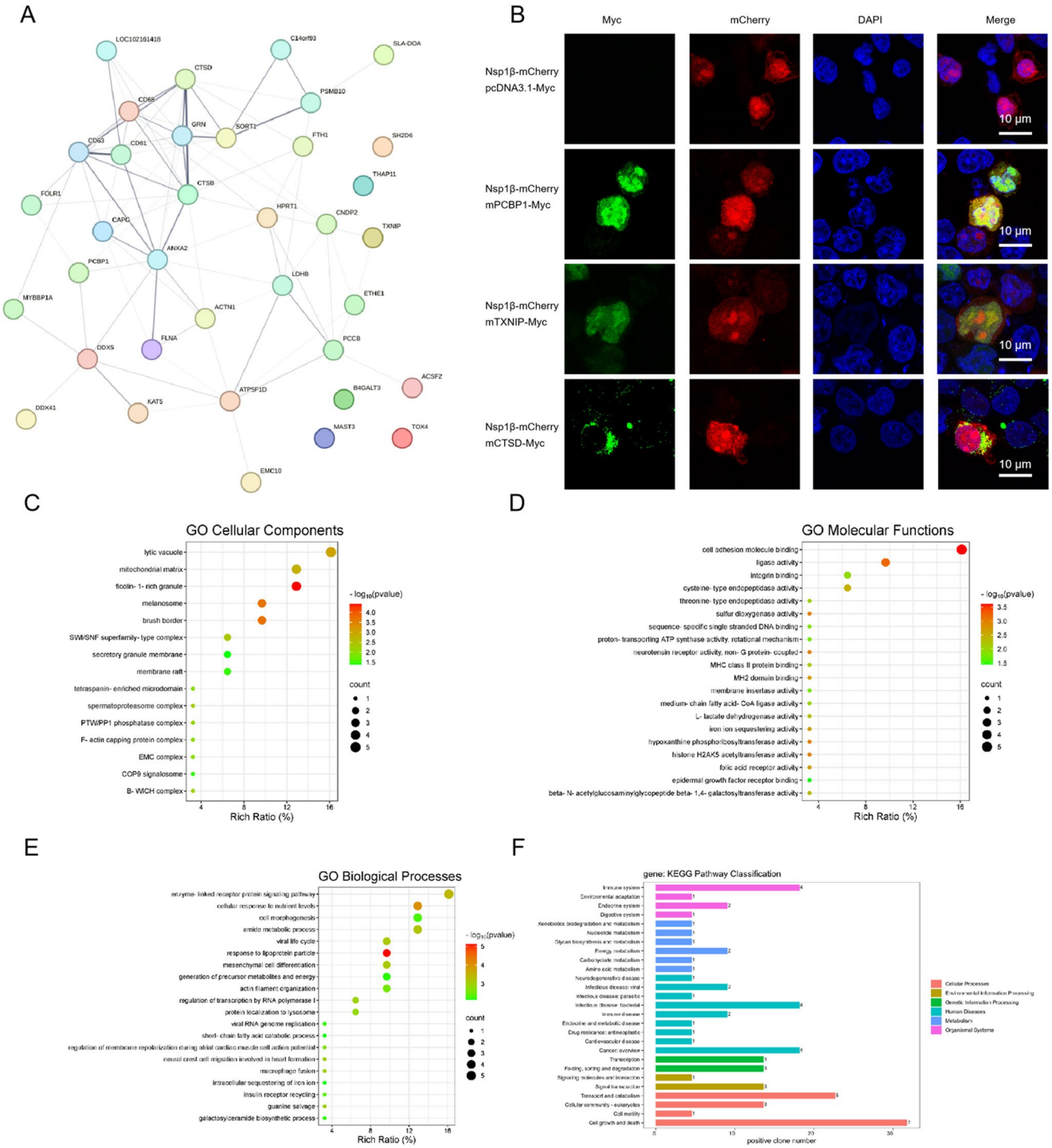

Fig. 2 Bioinformatics analysis and colocalization of interacting proteins. **(A)** Candidate host protein interaction network. **(B)** Confocal fluorescence microscopy confirmed the co-localization of Nsp1β with the host proteins PCBP1, TXNIP, and CTSD. HEK293 T cells were cotransfected with mPCBP1-Myc, mTXNIP-Myc, or mCTSD-Myc along with Nsp1β-mCherry plasmids. Myc empty vector and Nsp1β-mCherry were used as controls. At 24 hpt, the cells were subjected to indirect immunofluorescence analysis and visualized via confocal microscopy. Scale bars, indicated by white lines, represent the magnification. The "m" notation indicates that the species is a monkey. **(C)** GO cellular components analysis of the interacting proteins from Nsp1β bait screening, revealing the cellular locations where these proteins are likely to function. **(D)** GO molecular functions analysis of proteins interacting with Nsp1β, as identified via bait screening. This analysis highlights the molecular functions associated with the interaction partners. **(E)** GO biological processes analysis of the proteins interacting with Nsp1β, providing insights into the biological processes in which these proteins are involved. **(F)** KEGG pathway analysis of the interacting proteins from Nsp1β bait screening, outlining the key signaling pathways and processes in which these proteins may participate

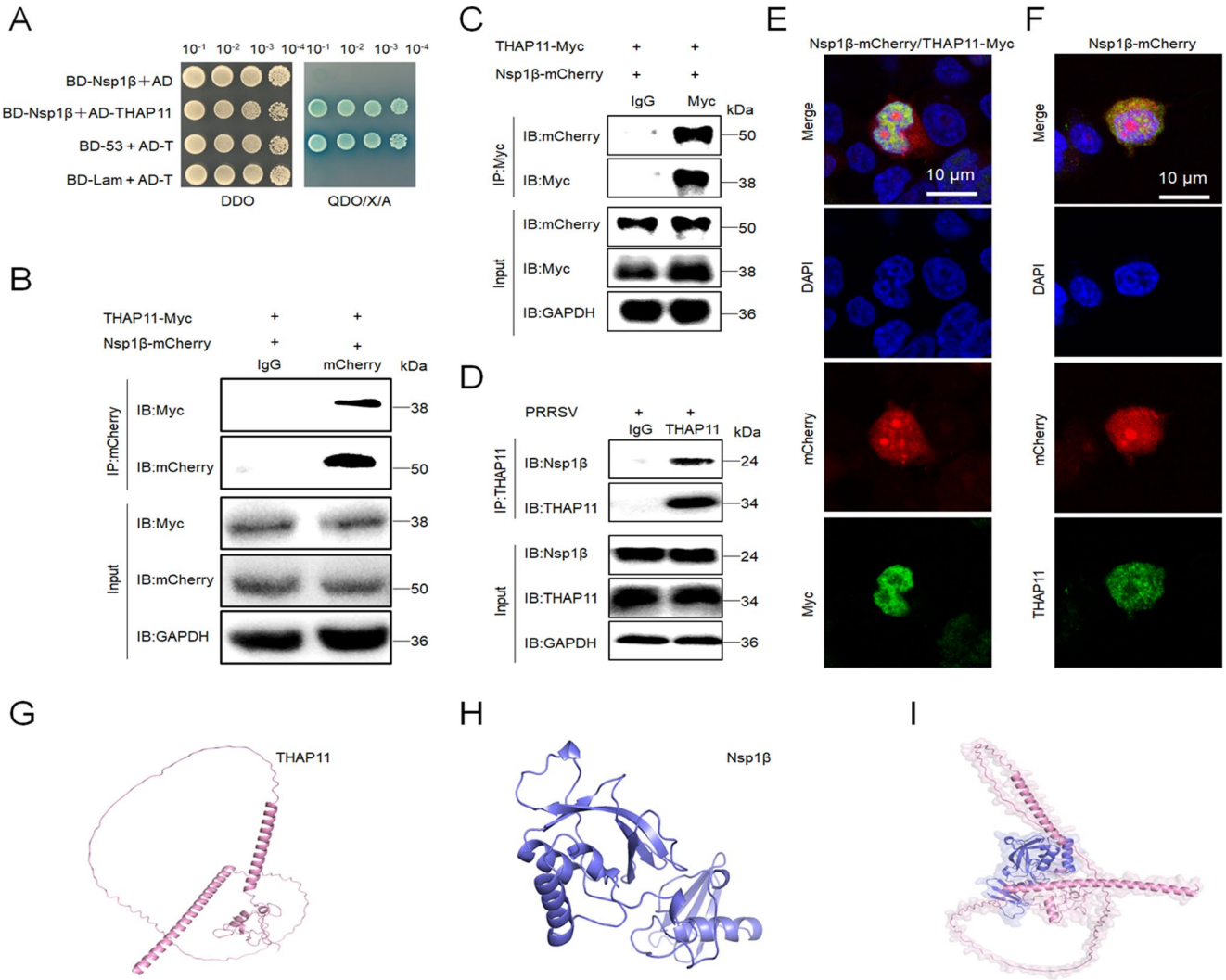

Fig. 3 Nsp1β interacts with THAP11. **(A)** Y2H assays confirmed the interaction between Nsp1β and THAP11. The pGBKT7-Nsp1β and pGADT7-THAP11 plasmids, or an empty vector, were cotransformed into Y2H Gold cells. pGBKT7-53 +pGADT7-T served as a positive control, and pGBKT7-Lam +pGADT7-T was used as a negative control. The transformed cells were grown on DDO and QDO/X/A media, with serial dilutions applied to assess the interaction. **(B)** Co-IP assays confirmed that Nsp1β interacts with THAP11. Anti-mCherry or anti-IgG antibodies were conjugated to magnetic A beads, and Myc-tagged proteins were detected in the immunoprecipitate. **(C)** Co-IP using anti-Myc antibodies conjugated to magnetic A beads detected the Nsp1β-mCherry protein in the immunoprecipitate, further supporting the interaction between Nsp1β and THAP11. **(D)** Co-IP assays confirmed the interaction between endogenous THAP11 and Nsp1β in PRRSV-infected Marc-145 cells. Anti-THAP11 antibodies linked to magnetic A beads were used to detect Nsp1β in the immunoprecipitate. **(E)** Cotransfection of Nsp1β-mCherry and THAP11-Myc into HEK293 T cells for 24 h resulted in co-localization of the two proteins, as observed by confocal fluorescence microscopy. **(F)** Transfection of Nsp1β-mCherry into HEK293 T cells for 24 h showed colocalization of the Nsp1β and endogenous THAP11, as observed by confocal fluorescence microscopy. **(G)** The predicted spatial structure of the monkey THAP11 protein, as determined by the AlphaFold3 server, reveals its folding pattern and key structural features. **(H)** The predicted spatial structure of Nsp1β, also obtained through AlphaFold3, shows the structural arrangement of this viral protein involved in immune modulation. **(I)** The predicted binding interface between Nsp1β and THAP11, as modeled by AlphaFold3, illustrates the potential interaction site, highlighting how these two proteins might interact at the molecular level. Pink stands for THAP11 protein spatial folding layers, and blue stands for Nsp1β protein spatial folding fragments

Co-IP results revealed that THAP11 could be detected in the immunoprecipitate (Fig. 3B), indicating an interaction between THAP11 and Nsp1β. Conversely, the anti-Myc antibody also strongly detected the Nsp1β-mCherry protein in the immunoprecipitate (Fig. 3C). Furthermore, endogenous THAP11 was immunoprecipitated with Nsp1β in PRRSV-infected Marc-145 cells via an anti-THAP11 antibody in a co-IP assay (Fig. 3D). Confocal fluorescence microscopy revealed overlapping yellow fluorescence in the cell nucleus when Nsp1β and THAP11 were coexpressed in HEK293 T cells, confirming the colocalization of Nsp1β with THAP11 (Fig. 3E). Moreover, immunofluorescence

microscopy revealed significant nuclear co-localization of viral Nsp1β with endogenous THAP11, suggesting potential functional interaction in this compartment (Fig. 3F). Collectively, these results confirm that Nsp1β interacts with THAP11 both in vivo and in vitro.

THAP11 is a transcriptional regulator containing a THAP domain. According to the AlphaFold3 prediction, the structure of THAP11 displays the characteristic THAP domain, which exhibits highly conserved secondary structural features, including β-sheets and α-helices, consistent with known structures of THAP family proteins. The protein features a tightly folded core, which is likely crucial for its roles in DNA and RNA binding, as well as transcriptional regulation (Fig. 3G). Nsp1β is a key protein of PRRSV that is known for its ability to disrupt host immune responses. The AlphaFold3 prediction indicated that Nsp1β adopts a highly folded structure containing multiple conserved α-helices and β-sheets (Fig. 3H). Through AlphaFold3 simulation of their interaction, the results suggest that THAP11 and Nsp1β likely bind through a network of hydrogen bonds and hydrophobic interactions, as indicated by a negative change in Gibbs free energy ($\Delta iG < 0$). The THAP-domain of THAP11 (Pink area) interacts with specific regions of Nsp1β (Blue area), forming a stable binding interface (Fig. 3I), which could influence the immune evasion mechanisms of PRRSV.

The predicted interaction structure provides molecular-level insights into THAP11-Nsp1β binding, contributing to a better understanding of the role of THAP11 in PRRSV infection and its impact on viral immune evasion.

THAP11 negatively regulates PRRSV replication

To investigate the relationship between THAP11 and PRRSV and understand the role of THAP11 during PRRSV infection, we first analyzed endogenous THAP11 expression in PRRSV-infected Marc-145 cells at 0, 6, 12, 24, and 36 h post-infection (hpi), with a multiplicity of infection (MOI) of 0.5. The results revealed that the accumulation of THAP11 protein did not significantly change at different time points following PRRSV infection (Fig. 4A). Marc-145 cells were subsequently transfected with either THAP11-Myc or an empty pcDNA3.1 vector for 12 h, after which PRRSV at an MOI of 0.5 was inoculated into the cells for 12, 24, or 36 h. The accumulation of the PRRSV N protein in the THAP11-Myc-expressing group was significantly lower than that in the control group (Fig. 4B), and qPCR analysis demonstrated significantly reduced N gene mRNA expression in THAP11-overexpressing cells at both 24 and 36 hpi (Fig. 4C). Consistent with transcriptional suppression, plaque assays revealed a corresponding reduction in viral titers from THAP11-expressing cells (Fig. 4D & E), indicating that exogenous expression of THAP11 inhibits PRRSV replication.

To further confirm the function of THAP11 during PRRSV infection, we performed siRNA-mediated RNA interference to knock down endogenous THAP11 expression. Two siRNAs targeting the THAP11 coding region (siTHAP11-1 and siTHAP11-2) were transfected into Marc-145 cells, with siNC (nontargeting control) used as a negative control. At 12 hpt, PRRSV was added to the cells and cultured for an additional 36 h. The expression of THAP11 was significantly lower in the siTHAP11 groups than in the siNC control group. The accumulation of the PRRSV ORF7 gene was upregulated more than twofold (Fig. 4F). Additionally, THAP11 protein levels were lower in the siRNA-silenced cells than in the siNC control cells. In contrast, the accumulation of the PRRSV N protein was significantly greater in the siTHAP11 groups (Fig. 4G), demonstrating that the knockdown of THAP11 facilitates PRRSV replication.

Furthermore, IFA revealed that, compared with the empty vector, THAP11 overexpression markedly reduced the fluorescence accumulation of the PRRSV N protein at both 12 and 24 hpi (Fig. 5A & B), and quantitative fluorescence intensity analysis confirmed this observation (Fig. 5C & D). In conclusion, these results suggest that THAP11 negatively regulates PRRSV replication.

THAP11 degrades Nsp1β via the ubiquitin-proteasome system

THAP11 has been reported to interact with PCBP1 to regulate transcription, suggesting that THAP11 may be a multifunctional protein. To explore the biological significance of its interactions, we constructed the plasmid pCAGGS-Nsp1β-HA, in which Nsp1β was fused with a C-terminal HA tag. Cotransfection of Nsp1β-HA and dose-independent THAP11-Myc plasmids into HEK293 T cells was performed. Protein analysis revealed that the accumulation of Nsp1β gradually decreased as THAP11 expression increased (Fig. 6A).

To clarify the degradation pathway, HEK293 T cells pretransfected with Nsp1β-HA and THAP11-Myc plasmids for 10 h were treated with the proteasome inhibitor MG132, the autophagy inhibitor 3-MA, or BafA1, with DMSO used as the control. Western blot analysis revealed that only the MG132-treated group retained Nsp1β protein accumulation, indicating that MG132 inhibited Nsp1β degradation (Fig. 6B). These findings suggest that THAP11 promotes Nsp1β degradation through the proteasome pathway.

Since proteasomal degradation requires ubiquitination, we next investigated whether Nsp1β could be modified by ubiquitination. HEK293 T cells were transfected with either Nsp1β-mCherry alone or in combination with Ub-HA for

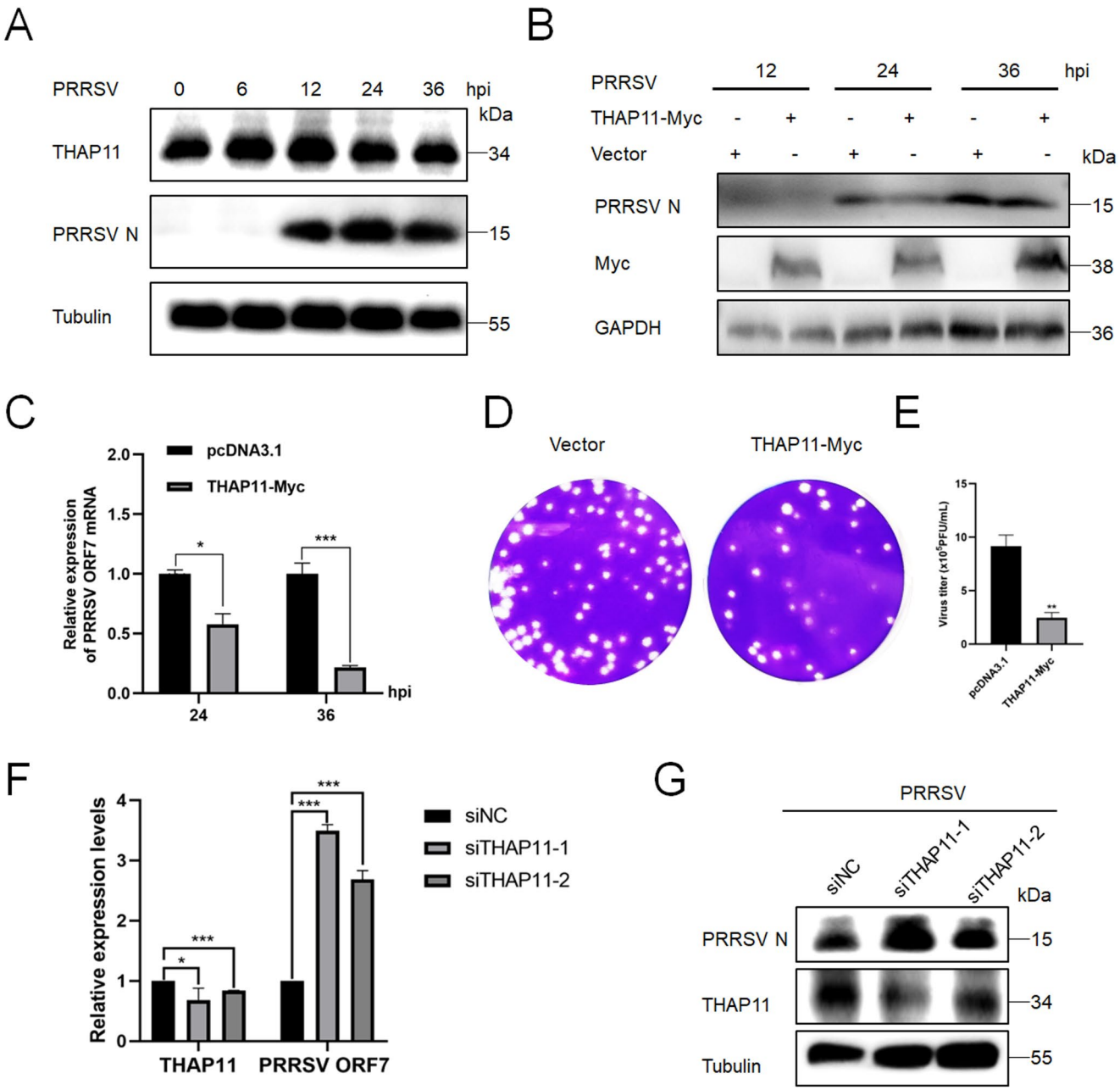

Fig. 4 THAP11 negatively regulates PRRSV infection. **(A)** Western blot analysis revealed endogenous THAP11 protein levels at different time points (0, 6, 12, 24, and 36 h) following PRRSV infection, revealing that THAP11 protein accumulation remained relatively stable throughout the infection. **(B & C)** Marc-145 cells were transfected with either 2 μg of THAP11-Myc or the pcDNA3.1 plasmid as a control. At 12 hpt, the cells were infected with PRRSV at an MOI of 0.5 for 12, 24, or 36 h. The accumulation of the PRRSV N protein was assessed via western blotting and relative expression of PRRSV ORF7 mRNA was analyzed by qPCR, which revealed reduced PRRSV replication in THAP11-Myc-expressing cells than in control cells. **(D & E)** Transfecting THAP11-Myc or empty vector plasmid into Marc-145 cells, the virus supernatant of 36 hpi was collected for plaque assay and virus titer analysis. **(F & G)** Knockdown of THAP11 enhanced PRRSV replication. Two siRNAs targeting THAP11 or a negative control siRNA were transfected into Marc-145 cells cultured in 12-well plates. At 12 hpt, the cells were infected with PRRSV for 36 h. The mRNA expression levels of THAP11 and the PRRSV ORF7 gene were measured via qPCR, and protein accumulation was analyzed via western blotting

24 h. Co-IP assays were used to analyze the ubiquitination levels of Nsp1β. Immunoprecipitation with an anti-mCherry antibody revealed a distinct ubiquitinated band in the cotransfection group, whereas single transfection did not result in any modified bands (Fig. 6C), confirming that Nsp1β can be ubiquitinated.

To determine whether THAP11 promotes Nsp1β ubiquitination and degradation, HEK293 T cells were

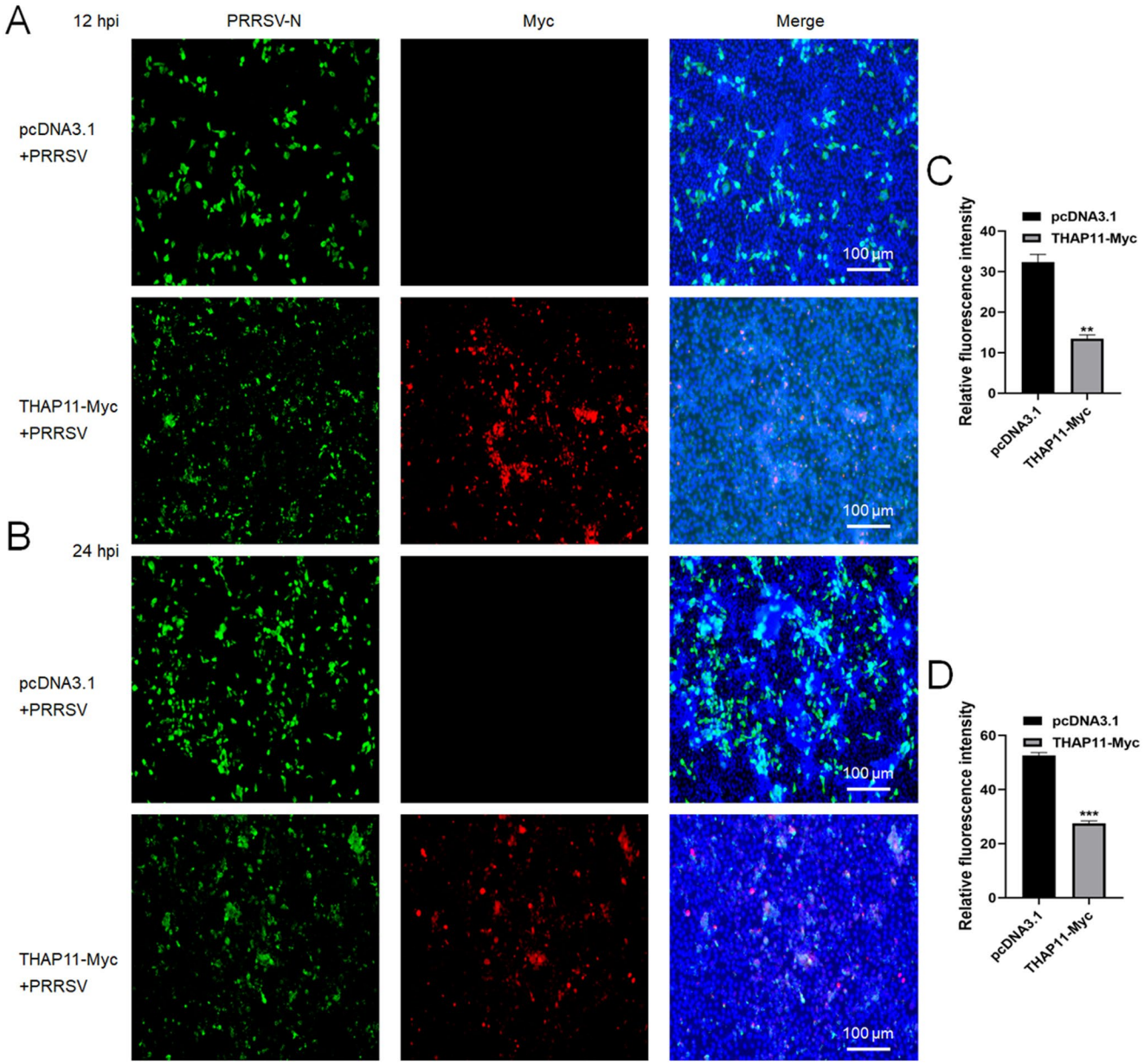

Fig. 5 IFA assays confirmed that THAP11 suppresses PRRSV replication. **(A & B)** Marc-145 cells were transfected with either THAP11-Myc or the pcDNA3.1 empty vector for 12 h, followed by PRRSV infection for 12–24 h. After the infection period, the cells were incubated overnight with the primary antibodies anti-N and anti-Myc. An anti-mouse 488 fluorescent secondary antibody was used to label the N protein, while an anti-rabbit 555 fluorescent secondary antibody was used to detect THAP11. Fluorescence images were captured via a Leica fluorescence microscope (Nikon, Germany), which revealed that THAP11 expression reduced PRRSV replication, as indicated by decreased N protein fluorescence. **(C & D)** Fluorescence count and luminance were statistically analyzed by Image J at 12 and 24 hpi

cotransfected with Nsp1β-mCherry, Ub-HA, or either an empty pcDNA3.1 vector or THAP11-Myc plasmid. At 24 hpt, the Co-IP results revealed that the level of ubiquitinated Nsp1β was significantly greater in cells expressing THAP11-Myc than in the control cells (Fig. 6D). Additionally, the ubiquitination levels increased in a dose-dependent manner (Fig. 6E). Collectively, these results indicate that THAP11 enhances the ubiquitination of Nsp1β, leading to its degradation via the proteasome.

THAP11 promotes K48- and K63-conjugated ubiquitination of Nsp1β for degradation

To further elucidate the type of ubiquitin conjugation involved in THAP11-mediated Nsp1β degradation, we focused on the ubiquitin-proteasome system, where K48- and K63-linked ubiquitin chains are generally associated with the degradation of misfolded proteins or pathogens. We constructed ubiquitin mutants retaining either the K6, K11,

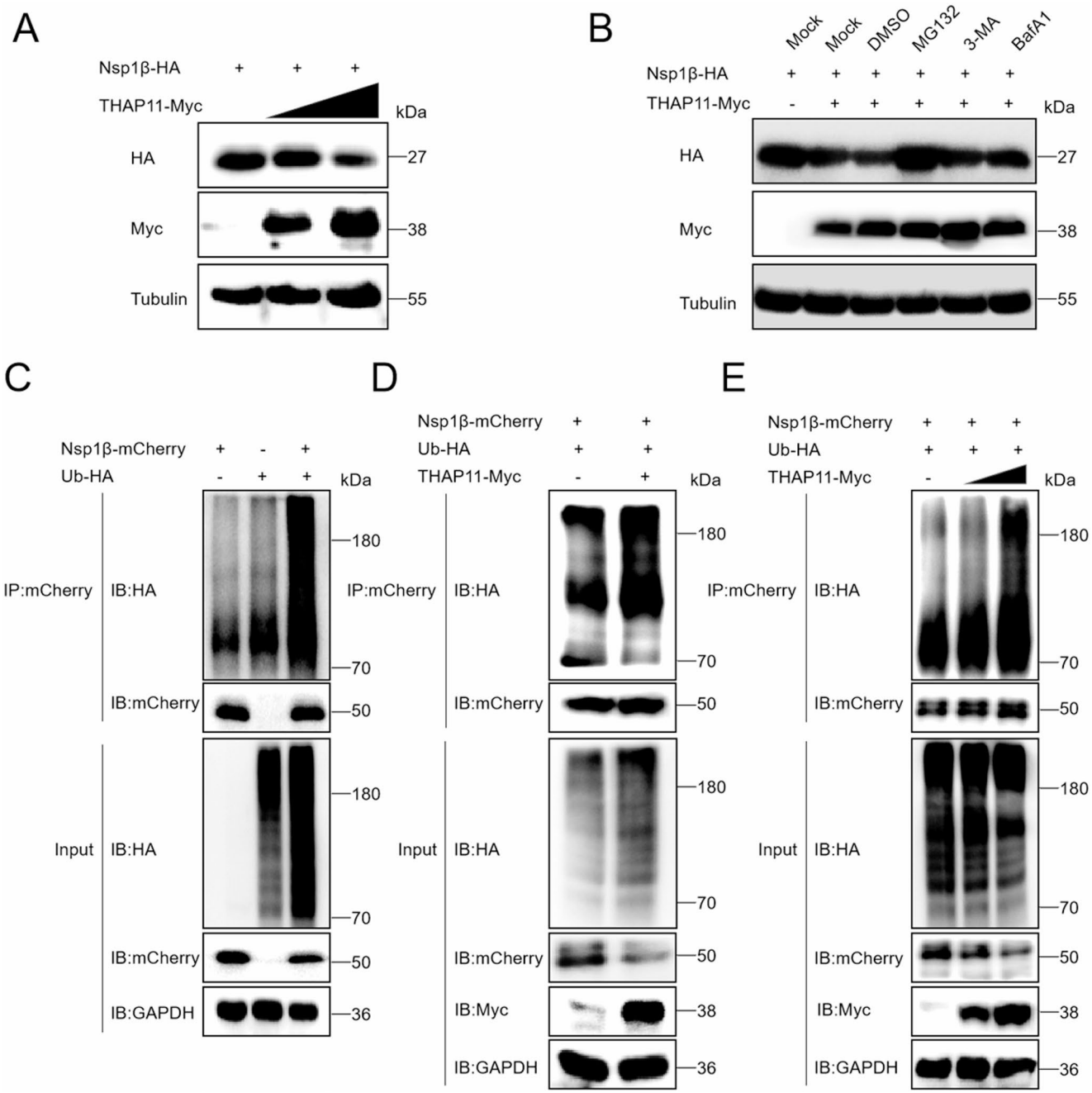

Fig. 6 THAP11 promotes Nsp1β ubiquitination and degradation via the ubiquitin-proteasome pathway. **(A)** HEK293 T cells were cotransfected with Nsp1β-HA and various doses (0, 1.0, or 1.5 μg) of THAP11-Myc plasmids. At 24 hpt, the accumulation of the Nsp1β protein was analyzed via western blotting, which revealed that the Nsp1β protein was regulated in a dose-dependent manner by THAP11. **(B)** A total of 2.0 μg of Nsp1β-HA and THAP11-Myc or empty vector was cotransfected into HEK293 T cells for 24 h. At 10 hpt, the cells were treated with the proteasome inhibitor MG132, the autophagy inhibitors 3-MA and BafA1, or DMSO as a control. Western blot analysis detected the accumulation of Nsp1β after 24 h. **(C)** HEK293 T cells were cotransfected with Nsp1β-mCherry and Ub-HA plasmids or with Nsp1β-mCherry or Ub-HA plasmids alone as controls. At 24 hpt, the degree of Nsp1β ubiquitination was detected via co-IP assays with an anti-HA antibody. An anti-mCherry antibody was linked to magnetic A beads for immunoprecipitation, confirming the ubiquitination of Nsp1β. **(D)** HEK293 T cells were cotransfected with Nsp1β-mCherry, Ub-HA, and THAP11-Myc or pcDNA3.1 plasmids. At 24 hpt, western blot analysis revealed increased ubiquitination of Nsp1β in the presence of THAP11, confirming its role in promoting Nsp1β ubiquitination. **(E)** HEK293 T cells were cotransfected with Nsp1β-mCherry, Ub-HA, or various doses of the THAP11-Myc plasmid. At 24 hpt, western blot analysis was used to detect the ubiquitination levels of Nsp1β

K27, K29, K33, K48 or K63 lysine site, as well as mutants where K48 or K63 was replaced with arginine (K48R or K63R), all in an HA-tagged vector. HEK293 T cells were co-transfected with Nsp1β-mCherry, THAP11-Myc or K6, K11, K27, K29, K33, K48, K63 or wild ubiquitin plasmids for 24 h, Co-IP result showed retaining K48 or K63 type ubiquitin has the similar ubiquitination levels as wild ubiquitin, indicating THAP11 mediated K48- and K63-linked ubiquitination type for Nsp1β degradation (Fig. 7A). To further confirm the result, HEK293 T cells were cotransfected with Nsp1β-mCherry, Ub(K48)-HA, and THAP11-Myc (or empty vector), as well as with Nsp1β-mCherry, Ub(K63)-HA, and THAP11-Myc (or empty vector). Co-IP analysis revealed that Nsp1β underwent significant ubiquitination when either the K48 or K63 lysine sites was retained in the ubiquitin molecule (Fig. 7B). Moreover, the expression of THAP11 further increased the levels of K48 and K63 ubiquitination in Nsp1β (Fig. 7C). Besides, inhibitor MG132 significantly rescued THAP11 mediate Nsp1β degradation via K48- or K63-linked ubiquitination and enhanced Nsp1β ubiquitination (Fig. 7D & E). These findings suggest that THAP11 promotes both K48- and K63-conjugated ubiquitination of Nsp1β, leading to its degradation.

Discussion

This study used a yeast two-hybrid system to screen for host proteins that interact with PRRSV Nsp1β and identified 34 potential interacting proteins. Among these, THAP11 strongly interacts with Nsp1β and was selected for further investigation. The overexpression of THAP11 significantly reduced PRRSV N protein accumulation, indicating antiviral activity, whereas the knockdown of THAP11 increased PRRSV replication. Importantly, THAP11 facilitated the degradation of Nsp1β by increasing K48- and K63-linked ubiquitination, thereby inhibiting PRRSV replication.

THAP11, a transcriptional regulator, may modulate host immune responses through its interaction with PRRSV Nsp1β. By reducing Nsp1β accumulation, the overexpression of THAP11 weakens the ability of the virus to evade the immune system and limits its replication. Conversely, THAP11 knockdown promoted Nsp1β accumulation, facilitating viral replication. Additionally, THAP11 mediates Nsp1β degradation via the ubiquitin-proteasome pathway, revealing the regulatory role of THAP11 during PRRSV infection.

This study is the first to reveal the interaction between THAP11 and PRRSV Nsp1β and its potential antiviral role. Previous studies have reported interactions between THAP11 and other host factors, such as PCBP1 and TXNIP, which play critical roles in transcription and cellular responses. However, the relationship between THAP11 and PRRSV has not been widely explored. This study fills this gap, suggesting that THAP11 may be involved in the host antiviral response through the ubiquitin-mediated degradation of Nsp1β.

While this study identified the potential antiviral role of THAP11, several limitations exist. First, the detailed mechanism by which THAP11 regulates Nsp1β degradation through ubiquitination remains to be fully elucidated and requires further experimental validation. Second, although the results observed in HEK293 T cells are promising and THAP11 derived from African green monkeys, pigs, humans and mice has 96.5% amino acid homology, whether these findings translate to in vivo pig models remains uncertain. TRIM29 promotes viral infection by suppressing type I interferon (IFN) production through MAVS-TBK1-IRF3 axis disruption and activating endoplasmic reticulum (ER) stress via PERK signaling [49–51]. We propose THAP11 counteracts these effects through two distinct mechanisms. On the one hand, as a THAP domain-containing transcription factor [32], it may bind the TRIM29 promoter to suppress its expression, thereby relieving IFN inhibition and restoring antiviral genes (e.g., ISG15, MX1) expression while also mitigating NLRP3 inflammasome suppression. On the other hand, through ER localization, THAP11 may independently modulate the unfolded protein response (e.g., via ATF4 regulation) to inhibit viral protein synthesis [33–37]. This dual regulatory capacity simultaneously enhances host immune responses while disrupting viral replication machinery, making THAP11 a potent multifunctional antiviral agent against PRRSV infection. In future research, we will explore these possible mechanisms in depth. Additionally, the roles of PCBP1, TXNIP, PSMB10, and CTSD in PRRSV infection need further confirmation through additional experiments.

Among the identified interacting proteins, PCBP1 has been shown to interact with PRRSV Nsp1β and play a key role in the lifecycle of several other viruses [38–42], indicating its potential importance in viral replication and immune modulation. In the context of hepatitis C virus (HCV) infection, PCBP1 is involved in stabilizing viral RNA and promoting its replication. Research has demonstrated that PCBP1 binds to the 5' untranslated region (UTR) of HCV RNA, stabilizing the RNA and facilitating its replication [40]. Similarly, PCBP1 has been implicated in regulating the translation of the SV40 large T antigen [43], further supporting its role as a multifunctional factor in viral processes. The influence of PCBP1 on viral RNA stability and replication is likely critical to the replication of many viruses. In the case of PRRSV, PCBP1 may influence the stability and transcription of viral RNA, potentially enhancing viral replication. Given that PRRSV relies on the host

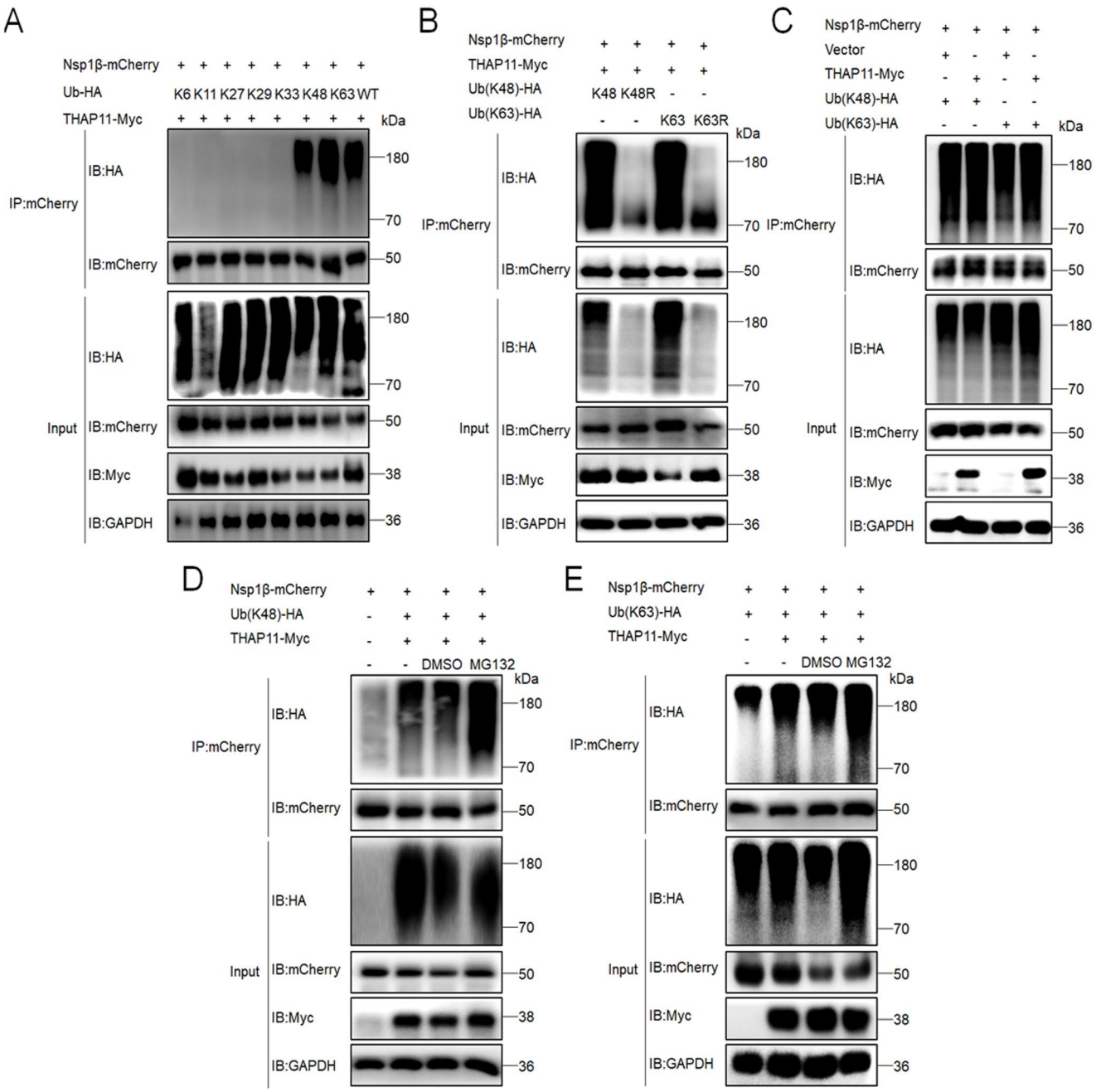

Fig. 7 THAP11-mediated Nsp1β degradation is dependent on K48- and K63-linked ubiquitination. **(A)** HEK293 T cells were co-transfected with Nsp1β-mCherry, THAP11-Myc, and ubiquitin mutants (K6, K11, K27, K29, K33, K48 or K63) or wild ubiquitin plasmids. At 24 hpt, western blot analysis detected Nsp1β ubiquitination levels, anti-mCherry was used in Co-IP assays. **(B)** HEK293 T cells were cotransfected with Nsp1β-mCherry, THAP11-Myc, or mutant Ub (K48, K48R, K63, or K63R) plasmids. At 24 hpt, western blot analysis was used to detect Nsp1β ubiquitination levels, and anti-mCherry was used in Co-IP assays. **(C)** HEK293 T cells were cotransfected with Nsp1β-mCherry, Ub(K48)-HA and THAP11-Myc or pcDNA3.1 plasmids or cotransfected with Nsp1β-mCherry, Ub(K63)-HA and THAP11-Myc or pcDNA3.1 plasmids. At 24 hpt, the degree of Nsp1β ubiquitination was detected via co-IP assays with an anti-HA antibody. mCherry antibody was coupled to magnetic A beads for immunoprecipitation. **(D & E)** HEK293 T cells were co-transfected with Nsp1β-mCherry, THAP11-Myc (empty vector control), and ubiquitin mutants (K48 or K63) plasmids. At 10 hpt, cells were treated with MG132 (10 μM) or DMSO for 14 h, western blot analysis detected Nsp1β ubiquitination levels, and anti-mCherry was used in Co-IP assays

cell machinery for RNA synthesis and stability, the interactions of PCBP1 with the viral genome could play a pivotal role in facilitating these processes. Future studies should explore the specific interactions between PCBP1 and the PRRSV genome to fully understand its contribution to viral replication. Understanding how PCBP1 regulates viral RNA could open new avenues for therapeutic intervention, particularly in modulating host-virus interactions to limit viral replication.

TXNIP has been studied extensively for its involvement in oxidative stress, inflammation, and immune-related pathways [44]. While direct evidence linking TXNIP to PRRSV is scarce, its broader role in viral infections and immune responses points to its potential relevance in PRRSV pathogenesis. TXNIP is known to regulate the NLRP3 inflammasome, which plays a pivotal role in triggering inflammatory pathways and pyroptosis under oxidative stress conditions [45]. This inflammasome activation could impact viral infections by modulating immune responses, including those observed in PRRSV infections. TXNIP has also been implicated in the regulation of apoptosis and redox balance, both of which influence viral replication and immune evasion [44]. TXNIP has been shown to regulate the cellular response during COVID-19 infection, where it inhibits oxidative stress in T cells, facilitating viral spread. TXNIP's role in viral replication is closely linked to its ability to modulate cellular redox states. By maintaining redox balance, TXNIP could create a more favorable environment for viral replication and immune evasion [46]. These findings suggest that TXNIP may help PRRSV manipulate host immune responses, suggesting an interesting avenue for future research on host-virus interactions. Further investigations are warranted to determine whether PRRSV influences TXNIP expression or activity, potentially contributing to its pathogenicity.

PSMB10, also known as MECL-1, is an integral component of the immunoproteasome and plays a crucial role in antigen processing for MHC class I presentation [52]. In response to interferon-gamma, PSMB10 replaces constitutive proteasome subunits in immune cells and assists in the degradation of viral proteins for immune recognition. This process is essential for the immune response during viral infection, and the immunoproteasome, including PSMB10, is involved in modulating pathways such as NF-κB signaling [53]. In viral infections such as classical swine fever virus, the proteasome, specifically PSMB10, processes viral proteins, promoting their recognition by the immune system [54]. These findings suggest that PSMB10 may play a role in PRRSV infection, potentially contributing to the degradation of viral proteins and enhancing immune system recognition.

CTSD, an aspartic protease located primarily in lysosomes, plays a significant role in various viral infections by facilitating different stages of the viral lifecycle. In viral contexts, the CTSD facilitates the processing of viral proteins, promotes viral entry, and triggers immune responses, such as antigen presentation [55]. For example, CTSD has been shown to activate viral glycoproteins after endocytosis, facilitating viral fusion with the host cell membrane [56, 57]. In infections such as SARS-CoV-2, the CTSD, along with other cathepsins such as B and L, is essential for cleaving the viral spike protein, which is crucial for viral entry into the host cell [58], highlighting the importance of CTSD in viral infections and suggests that it may play a similar role in PRRSV, potentially influencing viral entry and immune modulation. By expanding the understanding of how proteins such as TXNIP, PSMB10, and CTSD interact with viral proteins such as Nsp1β, this research opens new possibilities for exploring host-virus interactions in PRRSV and other viral infections. Further investigation into these pathways could lead to the development of targeted therapeutic strategies to modulate these interactions and combat PRRSV infections more effectively.

This study reveals, for the first time, that THAP11 inhibits PRRSV replication by interacting with and degrading Nsp1β via the ubiquitin-proteasome pathway. By revealing the interaction between THAP11 and Nsp1β, future studies will focus on exploring the role of THAP11 in other viral infections and whether it can be considered a broad-spectrum antiviral factor. Furthermore, given the interactions between PCBP1, TXNIP, and CTSD with PRRSV in this study, future work will further investigate the roles of these proteins in PRRSV infection and evaluate their potential as antiviral targets.

Supplementary Information The online version contains supplementary material available at https://doi.org/10.1007/s00018-025-05760-3.

Author contributions Binghua Chen: Writing-original draft, Data curation, Conceptualization, Formal analysis. Yongsheng Xie: Investigation, Methodology, Validation, Data curation. Zhan He: Software, Validation, Data curation. Yongjie Chen, Jiecong Yan, Fangfang Li, Yunyan Luo, Yanfei Pan and Min Liu: Validation, Data curation. Chunhe Guo: Conceptualization, Funding acquisition, Supervision, Writing-review & editing.

Funding This work was supported by the National Key Research and Development Program of China (2023YFD1801500), the Basic and Applied Basic Research Foundation of Guangdong Province (2024A1515012991), the Science and Technology Planning Project of Guangzhou (2023B03J0947 and 2025D04J0072), and the Laboratory of Lingnan Modern Agriculture Project (NG2022003).

Data availability The data will be made available upon request.

Declarations

Competing interest The authors declare that they have no conflicts of interest.

References

1. Lunney JK, Fang Y, Ladinig A, Chen N, Li Y, Rowland B, Renukaradhya GJ (2016) Porcine reproductive and respiratory syndrome virus (PRRSV): pathogenesis and interaction with the immune system. Annu Rev Anim Biosci 4:129–154
2. Kwon B, Ansari IH, Pattnaik AK, Osorio FA (2008) Identification of virulence determinants of Porcine reproductive and respiratory syndrome virus through construction of chimeric clones. Virology 380:371–378
3. Li Y, Wang X, Jiang P, Chen W, Wang X (2008) Genetic analysis of two Porcine reproductive and respiratory syndrome viruses with different virulence isolated in China. Arch Virol 153:1877–1884
4. Darwich L, Gimeno M, Sibila M, Diaz I, de la Torre E, Dotti S, Kuzemtseva L, Martin M, Pujols J, Mateu E (2011) Genetic and Immunobiological diversities of Porcine reproductive and respiratory syndrome genotype I strains. Vet Microbiol 150:49–62
5. Liu J, Wei C, Lin Z, Fan J, Xia W, Dai A, Yang X (2019) Recombination in lineage 1, 3, 5 and 8 of Porcine reproductive and respiratory syndrome viruses in China. Infect Genet Evol 68:119–126
6. Zhang Z, Zhang H, Luo Q, Zheng Y, Kong W, Huang L, Zhao M (2023) Variations in Nsp1 of Porcine reproductive and respiratory syndrome virus isolated in China from 1996 to 2022. Genes-basel 14:1435
7. Zhao HZ, Wang FX, Han XY, Guo H, Liu CY, Hou LN, Wang YX, Zheng H, Wang L, Wen YJ (2022) Recent advances in the study of NADC34-like Porcine reproductive and respiratory syndrome virus in China. Front Microbiol 13:950402
8. Ma J, Ma L, Yang M, Wu W, Feng W, Chen Z (2021) The function of the PRRSV-host interactions and their effects on viral replication and propagation in antiviral strategies. Vaccines-basel 9:364
9. Riccio S, Childs K, Jackson B, Graham SP, Seago J (2023) The identification of host proteins that interact with non-structural proteins-1alpha and–1beta of Porcine reproductive and respiratory syndrome virus-1. Viruses-basel 15:2445
10. Chen Z, Lawson S, Sun Z, Zhou X, Guan X, Christopher-Hennings J, Nelson EA, Fang Y (2010) Identification of two autocleavage products of nonstructural protein 1 (nsp1) in Porcine reproductive and respiratory syndrome virus infected cells: nsp1 function as interferon antagonist. Virology 398:87–97
11. Li Y, Tas A, Snijder EJ, Fang Y (2012) Identification of Porcine reproductive and respiratory syndrome virus ORF1a-encoded non-structural proteins in virus-infected cells. J Gen Virol 93:829–839
12. Song C, Krell P, Yoo D (2010) Nonstructural protein 1alpha subunit-based Inhibition of NF-kappaB activation and suppression of interferon-beta production by Porcine reproductive and respiratory syndrome virus. Virology 407:268–280
13. Han M, Du Y, Song C, Yoo D (2013) Degradation of CREB-binding protein and modulation of type I interferon induction by the zinc finger motif of the Porcine reproductive and respiratory syndrome virus nsp1alpha subunit. Virus Res 172:54–65
14. Han M, Kim CY, Rowland RRR, Fang Y, Kim D, Yoo D (2014) Biogenesis of non-structural protein 1 (nsp1) and nsp1-mediated type I interferon modulation in arteriviruses. Virology 458–459:136–150
15. Han M, Yoo D (2014) Modulation of innate immune signaling by nonstructural protein 1 (nsp1) in the family arteriviridae. Virus Res 194:100–109
16. Yuan S, Zhang N, Xu L, Zhou L, Ge X, Guo X, Yang H (2016) Induction of apoptosis by the nonstructural protein 4 and 10 of Porcine reproductive and respiratory syndrome virus. PLoS ONE 11:e0156518
17. Li Y, Shang P, Shyu D, Carrillo C, Naraghi-Arani P, Jaing CJ, Renukaradhya GJ, Firth AE, Snijder EJ, Fang Y (2018) Nonstructural proteins nsp2TF and nsp2N of Porcine reproductive and respiratory syndrome virus (PRRSV) play important roles in suppressing host innate immune responses. Virology 517:164–176
18. Contreras-Luna MJ, Fragoso-Gonzalez G, Segura-Velazquez RA, Cervantes-Torres JB, Alonso-Morales R, Ramirez-Martínez LA, Ayon-Nunez DA, Bobes RJ, Sanchez-Betancourt JI (2022) Immunogenic and antigenic analysis of Recombinant NSP1 and NSP11 of PRRS virus. Vet Med Sci 8:610–618
19. Beura LK, Sarkar SN, Kwon B, Subramaniam S, Jones C, Pattnaik AK, Osorio FA (2010) Porcine reproductive and respiratory syndrome virus nonstructural protein 1beta modulates host innate immune response by antagonizing IRF3 activation. J Virol 84:1574–1584
20. Kroese MV, Zevenhoven-Dobbe JC, Bos-de Ruijter JNA, Peeters BPH, Meulenberg JJM, Cornelissen LAHM, Snijder EJ (2008) The nsp1α and nsp1β papain-like autoproteinases are essential for Porcine reproductive and respiratory syndrome virus RNA synthesis. J Gen Virol 89:494–499
21. Li Y, Shyu DL, Shang P, Bai J, Ouyang K, Dhakal S, Hiremath J, Binjawadagi B, Renukaradhya GJ, Fang Y, Perlman S (2016) Mutations in a highly conserved motif of nsp1β protein attenuate the innate immune suppression function of Porcine reproductive and respiratory syndrome virus. J Virol 90:3584–3599
22. Xue F, Sun Y, Yan L, Zhao C, Chen J, Bartlam M, Li X, Lou Z, Rao Z (2010) The crystal structure of Porcine reproductive and respiratory syndrome virus nonstructural protein Nsp1β reveals a novel metal-dependent nuclease. J Virol 84:6461–6471
23. Han M, Ke H, Zhang Q, Yoo D (2017) Nuclear imprisonment of host cellular mRNA by nsp1β protein of Porcine reproductive and respiratory syndrome virus. Virology 505:42–55
24. Wang R, Nan Y, Yu Y, Zhang Y (2013) Porcine reproductive and respiratory syndrome virus Nsp1β inhibits interferon-activated JAK/STAT signal transduction by inducing karyopherin-α1 degradation. J Virol 87:5219–5228
25. Yang L, Zhang YJ (2017) Antagonizing cytokine-mediated JAK-STAT signaling by Porcine reproductive and respiratory syndrome virus. Vet Microbiol 209:57–65
26. Ke HZ, Han MY, Kim J, Gustin KE, Yoo DW (2019) Porcine reproductive and respiratory syndrome virus nonstructural protein 1 beta interacts with nucleoporin 62 to promote viral replication and immune evasion. J Virol 93:e00469–e00419
27. Zhai YY, Du YK, Yuan H, Fan S, Chen X, Wang J, He WR, Han SC, Zhang YH, Hu M, Zhang GP, Kong ZJ, Wan B (2024)

Ubiquitin-specific proteinase 1 stabilizes PRRSV nonstructural protein Nsp1β to promote viral replication by regulating K48 ubiquitination. J Virol 98:3
28. Pang Y, Zhou YR, Wang YC, Sun Z, Liu J, Li CY, Xiao SB, Fang LR (2022) Porcine reproductive and respiratory syndrome virus nsp1b stabilizes HIF-1a to enhance viral replication. Microbiol Spectr 10:e0317322
29. Su CM, Kim J, Tang J, Hung YF, Zuckermann FA, Husmann R, Roady P, Kim J, Lee YM, Yoo D (2024) A clinically attenuated double-mutant of Porcine reproductive and respiratory syndrome virus-2 that does not prompt overexpression of Proinflammatory cytokines during co-infection with a secondary pathogen. PLoS Pathog 20:e1012128
30. Li J, Wang D, Fang P, Pang Y, Zhou Y, Fang L, Xiao S (2022) DEAD-box RNA helicase 21 (DDX21) positively regulates the replication of Porcine reproductive and respiratory syndrome virus via multiple mechanisms. Viruses-basel 14:467
31. Gao P, Liu YY, Wang H, Chai Y, Weng WL, Zhang YN, Zhou L, Ge XN, Guo X, Han J, Yang HC (2022) Viral evasion of PKR restriction by reprogramming cellular stress granules. Proc Natl Acad Sci 119:29
32. Sanghavi HM, Mallajosyula SS, Majumdar S (2019) Classification of the human THAP protein family identifies an evolutionarily conserved coiled coil region. Bmc Struct Biol 19:7
33. Gervais V, Campagne S, Durand J, Muller I, Milon A (2013) NMR studies of a new family of DNA binding proteins: the THAP proteins. J Biomol Nmr 56:3–15
34. Lian WX, Yin RH, Kong XZ, Zhang T, Huang XH, Zheng WW, Yang Y, Zhan YQ, Xu WX, Yu M, Ge CH, Guo JT, Li CY, Yang XM (2012) THAP11, a novel binding protein of PCBP1, negatively regulates CD44 alternative splicing and cell invasion in a human hepatoma cell line. Febs Lett 586:1431–1438
35. Parker JB, Yin H, Vinckevicius A, Chakravarti D (2014) Host cell factor-1 recruitment to E2F-bound and cell-cycle-control genes is mediated by THAP11 and ZNF143. Cell Rep 9:967–982
36. Cukier CD, Maveyraud L, Saurel O, Guillet V, Milon A, Gervais V (2016) The C-terminal region of the transcriptional regulator THAP11 forms a parallel coiled-coil domain involved in protein dimerization. J Struct Biol 194:337–346
37. Ziaei S, Rezaei-Tavirani M, Ardeshirylajimi A, Arefian E, Soleimani M (2019) Induced overexpression of THAP11 in human fibroblast cells enhances expression of key pluripotency genes. Galen Med J 8:e1308
38. Beura LK, Dinh PX, Osorio FA, Pattnaik AK (2011) Cellular poly(C) binding proteins 1 and 2 interact with Porcine reproductive and respiratory syndrome virus nonstructural protein 1β and support viral replication. J Virol 85:12939–12949
39. Lu S, Luo Z, Dong X, Li Y, Zhang Q, Kim C, Song Y, Kang L, Liu Y, Wu K, Wu J (2014) PolyC-binding protein 1 interacts with 5′-untranslated region of enterovirus 71 RNA in membrane-associated complex to facilitate viral replication. PLoS ONE 9:e87491
40. Cousineau SE, Rheault M, Sagan SM (2022) Poly(rC)-binding protein 1 limits hepatitis C virus virion assembly and secretion. Viruses-basel 14:291
41. He HY, You Z, Ouyang T, Zhao G, Chen LJ, Wang Q, Li JY, Ye X, Zhang MH, Yang D, Ge XY, Qiu Y (2022) Poly(rC) binding protein 1 benefits coxsackievirus B3 infection via suppressing the translation of p62/SQSTM1. Virus Res 318:198851
42. Lee B, Chi X, Huang G, Wang L, Zhang X, Liu J, Yin Z, Guo G, Chen Y, Wang S, Chen JL (2024) A small protein encoded by PCBP1-AS1 is identified as a key regulator of influenza virus replication via enhancing autophagy. PLoS Pathog 20:e1012461
43. Su R, Kang X, Niu Y, Zhao T, Wang H (2024) PCBP1 interacts with the HTLV-1 tax oncoprotein to potentiate NF-κB activation. Front Immunol 15:1375168
44. Zhao Y, Chen Y, Liu Z, Zhou L, Huang J, Luo X, Luo Y, Li J, Lin Y, Lai J, Liu J (2024) TXNIP knockdown protects rats against bupivacaine-induced spinal neurotoxicity via the Inhibition of oxidative stress and apoptosis. Free Radical Bio Med 219:1–16
45. Yoshihara E, Matsuo Y, Masaki S, Chen Z, Tian H, Masutani H, Yamauchi A, Hirota K, Yodoi J (2024) Redoxisome update: TRX and TXNIP/TBP2-dependent regulation of NLRP-1/NLRP-3 inflammasome. Antioxid Redox Sign 40:10–12
46. Erkeland SJ, Palande KK, Valkhof M, Gits J, Oorschot ADV, Touw IP (2009) The gene encoding thioredoxin-interacting protein (TXNIP) is a frequent virus integration site in virus-induced mouse leukemia and is overexpressed in a subset of AML patients. Leuk Res 33:1367–1371
47. Yuan Y, Fang A, Zhang M, Zhou M, Fu ZF, Zhao L (2024) Lassa virus Z protein hijacks the autophagy machinery for efficient transportation by interrupting CCT2- mediated cytoskeleton network formation. Autophagy 20:2511–2528
48. Pan WW, Long J, Xing JJ, Zheng CF (2011) Molecular determinants responsible for the subcellular localization of HSV-1 UL4 protein. Virol Sin 25:347–356
49. Xing J, Zhang A, Minze LJ, Li XC, Zhang Z (2018) TRIM29 negatively regulates the type I IFN production in response to RNA virus. J Immunol 201:183–192
50. Wang J, Lu W, Zhang J, Du Y, Fang M, Zhang A, Sungcad G, Chon S, Xing J (2024) Loss of TRIM29 mitigates viral myocarditis by attenuating PERK-driven ER stress response in male mice. Nat Commun 15:3481
51. Wang J, Wang L, Lu W, Farhataziz N, Gonzalez A, Xing J, Zhang Z (2025) TRIM29 controls enteric RNA virus-induced intestinal inflammation by targeting NLRP6 and NLRP9b signaling pathways. Mucosal Immunol 18:135–150
52. Schwarz K, van den Broek M, Kostka S, Kraft R, Soza A, Schmidtke G, Kloetzel PM, Groettrup M (2000) Overexpression of the proteasome subunits LMP2, LMP7, and MECL-1, but not PA28α/β, enhances the presentation of an immunodominant lymphocytic choriomeningitis virus T cell epitope. J Immunol 165:768–778
53. Li J, Wang S, Bai J, Yang XL, Zhang YL, Che YL, Li HH, Yang YZ (2018) Novel role for the Immunoproteasome subunit PSMB10 in angiotensin II–induced atrial fibrillation in mice. Hypertension 71:866–876
54. Deng S, Yang C, Nie K, Fan S, Zhu M, Zhu J, Chen Y, Yuan J, Zhang J, Xu H, Tian S, Chen J, Zhao M (2019) Host cell protein PSMB10 interacts with viral NS3 protein and inhibits the growth of classical swine fever virus. Virology 537:74–83
55. Messaoudi KE, Thiry LF, Liesnard C, Tieghem NV, Bollen A, Moguilevsky N (2000) A human milk factor susceptible to cathepsin D inhibitors enhances human immunodeficiency virus type 1 infectivity and allows virus entry into a mammary epithelial cell line. J Virol 74:1004–1007
56. Hasui K, Wang J, Jia X, Tanaka M, Nagai T, Matsuyama T, Eizuru Y (2011) Enhanced autophagy and reduced expression of cathepsin D are related to autophagic cell death in epstein-barr virus-associated nasal natural killer/T-cell lymphomas: an immunohistochemical analysis of beclin-1, LC3, mitochondria (AE-1), and cathepsin D in nasopharyngeal lymphomas. Acta Histochem Cytoc 44:119–131
57. Wang Y, Han H, Zhu K, Xu S, Han C, Jiang Y, Wei S, Qin Q (2022) Functional analysis of the cathepsin D gene response to SGIV infection in the orange-spotted Grouper, epinephelus coioides. Viruses-basel 14:1680

58. Shirvaliloo M (2022) The unfavorable clinical outcome of COVID-19 in smokers is mediated by H3K4me3, H3K9me3 and H3K27me3 histone marks. Epigenomics-uk 14:153–162